Differential Interfacial and Substrate Binding Modes of Mammalian Pancreatic Phospholipases A_2: A Comparison among Human, Bovine, and Porcine Enzymes[†]

Yana Snitko, Sang Kyou Han, Byung In Lee, and Wonhwa Cho*

Department of Chemistry (M/C 111), University of Illinois at Chicago, 845 West Taylor Street, Chicago, Illinois 60607-7061

Received March 16, 1999; Revised Manuscript Received April 22, 1999

ABSTRACT: To identify the residues essential for interfacial binding and substrate binding of human pancreatic phospholipase A_2 (hpPLA_2), several ionic residues in the putative interfacial binding surface (R6E, K7E, K10E, and K116E) and substrate binding site (D53K and K56E) were mutated. Interfacial affinity of these mutants was measured using anionic polymerized liposomes, and their enzymatic activity was measured using various substrates including phospholipid monomers, zwitterionic and anionic micelles, and anionic polymerized mixed liposomes. Similar mutations (R6E, K10E, K56E, and K116E) were made to porcine pancreatic phospholipase A_2 (ppPLA_2), and the properties of mutants were measured by the same methods. Results indicate that hpPLA_2 and ppPLA_2 have similar interfacial binding mechanisms in which cationic residues in the amino terminus and Lys-116 in the carboxy terminus are involved in binding to anionic lipid surfaces. Small but definite differences between the two enzymes were observed in overall interfacial affinity and activity and the effects of the mutations on interfacial enzyme activity. The interfacial binding of hpPLA_2 and ppPLA_2 is distinct from that of bovine pancreatic phospholipase A_2 in that Lys-56 is involved in the interfacial binding of the latter enzyme. The unique phospholipid headgroup specificity of hpPLA_2 derives from the presence of Asp-53 in the substrate binding site. This residue appears to participate in stabilizing electrostatic interactions with the cationic ethanolamine headgroup, hence the phosphatidylethanolamine preference of hpPLA_2. Taken together, these studies reveal the similarities and the differences in the mechanisms by which mammalian pancreatic phospholipases A_2 interact with lipid aggregates and perform interfacial catalysis.

Phospholipases A_2 (PLA_2)[1] catalyze the hydrolysis of the fatty acid ester in the *sn*-2 position of phospholipids to produce a fatty acid and a lysophospholipid. PLA_2s are a large family of enzymes that are found both in intracellular and in secreted forms (*1*). Mammalian pancreatic PLA_2s (group Ib) are highly homologous proteins the main function of which is to digest dietary phospholipids emulsified with bile (*2*). Several lines of evidence have indicated that mammalian pancreatic PLA_2s are also present in different tissues and might be involved in the receptor-mediated regulation of cellular functions (*3*).

Since PLA_2 acts on phospholipids in membranes or in other aggregated forms, the reaction cycle includes the interfacial binding which is distinct from the binding of a phospholipid molecule to the active site (*4*, *5*). Structural (*6*, *7*) and mutational (*8*−*10*) analyses of several secretory PLA_2s have indicated that they have an interfacial binding surface (IBS) that is topologically distinct from the active site. Due to the presence of separate IBS and active site, PLA_2 displays two types of substrate specificity: the substrate specificity of the active site and the interfacial preference of the IBS (*8*, *10*, *11*). Since secretory PLA_2s show little *sn*-2 acyl group specificity, their substrate specificity usually refers to the phospholipid headgroup specificity. We have recently shown that despite their high sequence homology bovine (bpPLA_2), porcine (ppPLA_2), and human pancreatic PLA_2 (hpPLA_2) have distinct phospholipid headgroup specificity and interfacial preference (*12*).

Extensive structure−function studies on bpPLA_2 (*8*, *9*, *13*) and ppPLA_2 (*14*, *15*) have identified the protein residues involved in their interfacial binding and substrate specificity. To identify the hpPLA_2 residues that are involved in its substrate and interfacial binding and also to understand the origin of the differential substrate specificity and interfacial preference of the three pancreatic PLA_2s, we performed the systematic mutagenesis of hpPLA_2 and ppPLA_2, and measured the effects of mutations on their kinetic and membrane binding properties. In conjunction with our previous structure−function studies on bpPLA_2, these studies provide the first detailed information about the similarities and differences in the mechanisms by which mammalian pancreatic PLA_2s

[†] This work was supported by National Institutes of Health Grants GM52598 and GM53987. W.C. is an Established Investigator of the American Heart Association.

* To whom correspondence should be addressed. Telephone: 312-996-4883. Fax: 312-996-2183. E-mail: wcho@uic.edu.

[1] Abbreviations: BLPG, 1,2-bis[12-(lipoyloxy)dodecanoyl]-*sn*-glycero-3-phosphoglycerol; bpPLA_2, bovine pancreatic PLA_2; BSA, bovine serum albumin; CD, circular dichroism; diC_8PC, 1,2-dioctanoyl-*sn*-3-phosphocholine; diC_8PE, 1,2-dioctanoyl-*sn*-glycero-3-phosphoethanolamine; diC_6PG, 1,2-dihexanoyl-*sn*-glycero-3-phosphoglycerol; HEPES, *N*-(2-hydroxyethyl)piperazine-*N*′-2-ethanesulfonic acid; hpPLA_2, human pancreatic PLA_2; IBS, interfacial binding surface; PC, phosphatidylcholine; PE, phosphatidylethanolamine; PG, phosphatidylglycerol; PLA_2, phospholipase A_2; ppPLA_2, porcine pancreatic PLA_2; pyrene-PE, 1-hexadecanoyl-2-(1-pyrenedecanoyl)-*sn*-glycero-3-phosphoethanolamine; pyrene-PG, 1-hexadecanoyl-2-(1-pyrenedecanoyl)-*sn*-glycero-3-phosphoglycerol; SDS, sodium dodecyl sulfate.

10.1021/bi990600e CCC: $18.00
Published on Web 05/26/1999

interact with lipid aggregates and perform interfacial catalysis.

MATERIALS AND METHODS

Materials. 1-Hexadecanoyl-2-(1-pyrenedecanoyl)-*sn*-glycero-3-phosphoethanolamine (pyrene-PE) and -glycerol (pyrene-PG) were purchased from Molecular Probes (Eugene, OR). 1,2-Dihexanoyl-*sn*-3-phosphoglycerol (diC_6PG), 1,2-dioctanoyl-*sn*-3-phosphoethanolamine (diC_8PE), and 1,2-dioctanoyl-*sn*-3-phosphocholine (diC_8PC) were from Avanti Polar Lipids, Inc. (Alabaster, AL). 1,2-Bis[12-(lipoyloxy)-dodecanoyl]-*sn*-glycero-3-phosphoglycerol (BLPG) was prepared as described (*11*). Large unilamellar liposomes of BLPG were prepared by multiple extrusion of phospholipid dispersion in 10 mM Tris-HCl buffer (pH 8.4) through a 0.1-μm polycarbonate filter (Millipore) in a Liposofast microextruder (Avestin, Ottawa, Ontario) and then polymerized in the presence of 10 mM dithiothreitol as described (*16*). Phospholipid concentrations were determined by phosphate analysis (*17*). Triton X-100, sodium deoxycholate, and dodecylsucrose were from Pierce (Rockford, IL), Sigma, and Calbiochem (San Diego, CA), respectively. Fatty acid-free bovine serum albumin (BSA) was from Bayer Inc. (Kankakee, IL). 5,5′-Dithiobis(2-nitrobenzoic acid) and sodium sulfite were obtained from Aldrich. 2-Nitro-5-(sulfothio)-benzoate was synthesized from 5,5′-dithiobis(2-nitrobenzoic acid) as described by Thannhauser et al. (*18*). All restriction enzymes, T4 ligase, T4 polynucleotide kinase, and isopropyl β-D-thiogalactopyranoside were obtained from Boehringer Mannheim Biochemicals. Oligonucleotides were purchased from Integrated DNA Technologies (Coralville, IA) and used without further purification. Recombinant $bpPLA_2$ was prepared as described previously (*8*).

Mutagenesis of $hpPLA_2$ and $ppPLA_2$. The synthetic gene for $hpPLA_2$ (*12*) was subcloned into the pET-21a vector (Novagen, Madison, WI), and the construct was designated pSH-hp. The coding region of the $ppPLA_2$ gene was kindly provided by Prof. H. M. Verheij of Utrecht University. It was subcloned into the pET-21a vector, and the construct was designated pBL-pp. The mutagenesis was performed using a Sculptor in vitro mutagenesis kit from Amersham−Pharmacia as described (*10*). The oligonucleotides used for the construction of $hpPLA_2$ mutants were 5′-CTT GAT CAT CTT CTC GAA CTG CCA AAC-3′ (R6E), 5′-GCA CTT GAT CAT CTC GCG GAA CTG CCA AAC-3′ (K7E), 5′-GG AAT AAC GCA CTC GAT CAT CTT GCG G-3′ (K10E), 5′-CTT CTT CGC TTG *CTT* GTA GCA GTT GTC-3′ (D53K), 5′-CT GTC CAG CTT CTC CGC TTG ATC GTA G-3′ (K56E), and 5′-GT GTC CAG GTT CTC GTG TGC CTT GTT A-3′ (K116E). The oligonucleotides used for $ppPLA_2$ mutations were 5′- CTT AAT CAT GCT TTC AAA CTG CCA TAA-3′ (R6E), 5′-GGG GAT TGC GCA CTC AAT CAT GCT ACG-3′ (K10E), 5′-GCT GTC CAG GTT CTC GGC ATC TCT GTA-3′ (K56E), and 5′-GGT GTC CAG GTT CTC GTG CTC CTT GTT-3′ (K116E). The underlined bases indicate the location of charge-reversal mutations. After the DNA sequences of the entire coding regions of mutants were verified using a Sequenase 2.0 kit (Amersham-Pharmacia), individual mutant pSH-hp and pBL-pp vectors were transformed into an *Escherichia coli* strain, BL21(DE3), for protein expression.

Expression and Purification of Mammalian Pancreatic PLA_2s. Recombinant $hpPLA_2$ (*12*), $bpPLA_2$ (*8*), and $ppPLA_2$ (*8*) were expressed in *E. coli* and purified as described previously. The purity of protein was confirmed by SDS−polyacrylamide electrophoresis. Protein concentrations were determined by the bicinchoninic acid method (Pierce). The circular dichroism (CD) spectra of proteins were measured in 10 mM phosphate buffer, pH 7.4, at 25 °C using a Jasco J-600 spectropolarimeter. Each spectrum was obtained at wavelengths between 190 and 300 nm and averaged from 10 separate scans.

Measurements of Protein Stability. The thermodynamic stability of wild-type and mutant proteins was measured from their equilibrium denaturation by guanidinium chloride. Briefly, proteins were incubated in 10 mM phosphate buffer, pH 7.4, containing 0−8 M guanidinium chloride for 2 h at 25 °C and their CD spectra measured. Assuming that the protein folding follows the two-state model (i.e., native ↔ unfolded), the molar ellipticity values at 222 nm (θ_{222}) at different guanidinium chloride concentrations were converted to the fraction of unfolded protein (f_u) using the equation: $f_u = (\theta_N - \theta_{222})/(\theta_N - \theta_U)$ where θ_N and θ_U are the extrapolated base lines for the native and unfolded protein, respectively (*19*, *20*). The free energy of folding (ΔG_{fold}) was determined from the nonlinear least-squares analysis of the f_u vs [guanidinium chloride] plot using the equation:

$$f_u = 1/\left\{1 + \exp - \left[\frac{\Delta G_{fold}}{RT} + \frac{m[\text{guanidinium chloride}]}{RT}\right]\right\}$$

where m indicates the slope of the plot in the transition region.

Kinetic Measurements. The PLA_2-catalyzed hydrolysis of polymerized mixed liposomes was carried out at 37 °C in 2 mL of 10 mM HEPES buffer, pH 7.4, containing 0.1 μM pyrene-labeled phospholipids (1 mol %) inserted in 9.9 μM BLPG, 2 μM BSA, 0.16 M NaCl, and 10 mM $CaCl_2$. The progress of hydrolysis was monitored fluorometrically, and the rate constant was calculated from the nonlinear least-squares analysis of the reaction progress curve as described previously (*8*, *11*, *16*). The PLA_2-catalyzed hydrolysis of diC_6PG monomers and diC_8PC micelles was measured in the presence of 0.5 mM phospholipid, 0.16 M NaCl, and 10 mM $CaCl_2$ at 37 °C. The hydrolysis of mixed micelles was measured in the presence of 2 mM Triton X-100, 1 mM sodium deoxycholate, 0.5 mM diC_8PE, 0.16 M NaCl, and 10 mM $CaCl_2$ as described previously (*21*). The time course of phospholipid hydrolysis was monitored with a computer-controlled Metrom pH stat (Brinkmann) in a thermostated vessel. Under these conditions, the hydrolysis of diC_6PG, diC_8PE, and diC_8PC followed first-order kinetics because the substrate concentrations remained lower than the apparent K_M values. Thus, the pseudo-first-order rate constants were determined from the nonlinear least-squares analysis of the reaction progress curves. The values of $(k_{cat}/K_M)_{app}$ were calculated by dividing the pseudo-first-order rate constants by the enzyme concentrations.

Binding of Pancreatic PLA_2s to Sucrose-Loaded Polymerized Liposomes. The binding of pancreatic PLA_2s to sucrose-loaded polymerized liposomes was measured by a centrifugation method as described previously (*22*). The sucrose-loaded BLPG liposomes (100 nm diameter) were

prepared in 10 mM Tris-HCl buffer, pH 8.4, containing 0.32 M sucrose and polymerized for 30 h at 37 °C in the presence of 10 mM dithiothreitol. Nonentrapped sucrose molecules were removed by the gel-filtration chromatography using a Sephadex G-25 column equilibrated and eluted with 10 mM Tris-HCl buffer, pH 7.4, containing 0.16 M NaCl. For binding measurements, 500 μL aliquots of 100 μM of BLPG-polymerized liposomes were incubated with 0.03−0.5 μM (for $hpPLA_2$) and 0.03−2 μM (for $ppPLA_2$) aliquots of the protein solution in 10 mM Tris-HCl buffer, pH 7.4, containing 0.145 M NaCl, 10 mM $CaCl_2$, and 1 μM BSA for 30 min at 37 °C. For weak vesicle binding mutants (e.g., R6E and K116E of $hpPLA_2$ and $ppPLA_2$), higher vesicle concentrations were used (i.e., 200−300 μM). The mixtures were then centrifuged for 20 min at 100000*g* and at 25 °C using a Sorvall RCM120EX microultracentrifuge equipped with a S120AT3 rotor (Sorvall) to pellet the polymerized liposomes. After centrifugation, the concentration of free enzyme ($[E]_f$) in the supernatant was determined by measuring the PLA_2 activity toward pyrene-PG/BLPG polymerized mixed liposomes as described above. The bound PLA_2 concentration ($[E]_b$) was plotted as a function of $[E]_f$, and the values of n and K_d were determined by the nonlinear least-squares analysis of the $[E]_b$ versus $[E]_f$ plot using the standard Langmuir-type binding equation:

$$[E]_b = ([BLPG]T/n)/(1 + K_d/[E]_f) \quad (1)$$

where $[BLPG]_T$ represents the total BLPG concentration. Equation 1 assumes that each enzyme binds independently to a site on the interface composed of n phospholipids and with the dissociation constant K_d.

RESULTS

Design and Physical Properties of Mutants. We previously showed that $hpPLA_2$ has unique phospholipid headgroup specificity and interfacial preference (*12*). To identify the $hpPLA_2$ residues that are involved in its substrate and interfacial binding, we generated a series of mutants for $hpPLA_2$. The design of mutants was based on our previous finding on $bpPLA_2$ (*8*, *9*) and other secretory PLA_2s (*10*, *22*, *23*): Their interfacial binding to anionic interfaces is driven in large part by cationic side chains on their IBS (e.g., Lys-10, Lys-56, and Lys-116 for $bpPLA_2$), and the substrate headgroup specificity is governed in part by ionic side chains of residues 53−58 (e.g., Lys-53 and Lys-56 for $bpPLA_2$). Accordingly, we replaced three cationic residues in the amino terminus of $hpPLA_2$ (Arg-6, Lys-7, Lys-10), as well as Lys-56 and Lys-116, with glutamate. We also mutated Asp-53 to lysine. Similar mutations were performed for $ppPLA_2$ (i.e., R6E, K10E, K56E, and K116E) for comparison. Because the mutated side chains of $hpPLA_2$ and $ppPLA_2$ are largely solvent-exposed, they did not have significant effects on protein structure and stability. For both $hpPLA_2$ and $ppPLA_2$, most of the mutant proteins were expressed and refolded as efficiently as wild type (data not shown), and their CD spectra were similar (Figure 1). The thermodynamic stability of wild type and mutants was also comparable for both $hpPLA_2$ and $ppPLA_2$. As shown in Figure 2, the guanidinium chloride-induced denaturation curves of wild type and selected mutants are essentially the same for both $hpPLA_2$ and $ppPLA_2$: $\Delta G°_{fold} = 9.0 \pm 2.0$ kcal/mol for $hpPLA_2$ and its K116E mutant and $\Delta G°_{fold} = 6.7 \pm 1.5$ kcal/mol for $ppPLA_2$ and its K116E mutant. Other mutants of $hpPLA_2$ and $ppPLA_2$ also behaved similarly to the K116E mutants (data not shown).

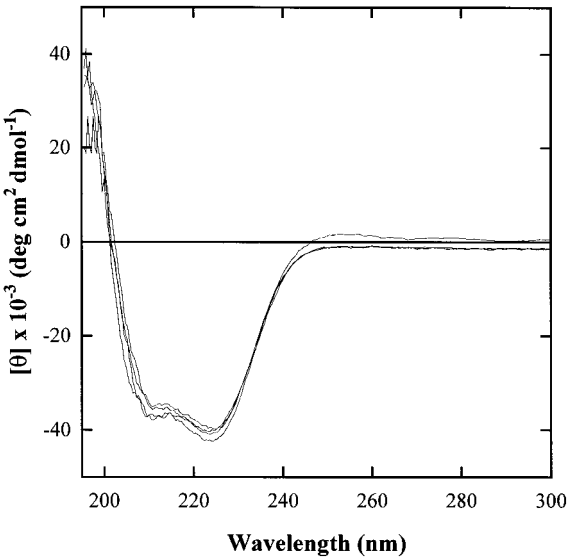

FIGURE 1: Circular dichroism spectra of human pancreatic PLA_2 and selected mutants including R6E, K56E, and K116E. The concentrations of proteins were 25 μM in 0.01 M phosphate buffer, pH 7.4. The spectra of other $hpPLA_2$ mutants, $ppPLA_2$, and its mutants are similar.

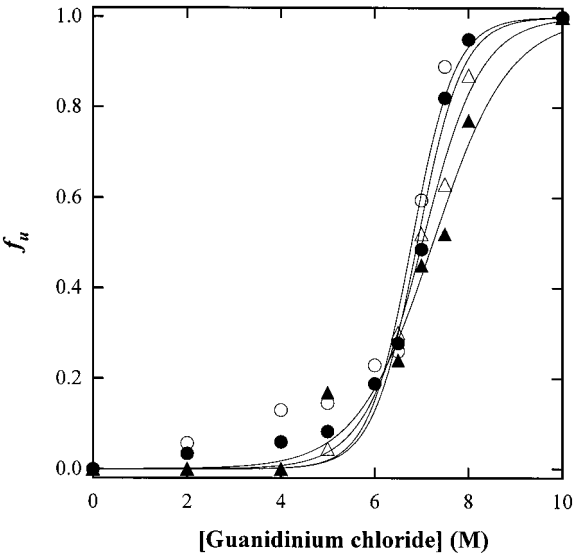

FIGURE 2: Guanidinium chloride-induced unfolding of human pancreatic PLA_2 (○), human K116E mutant (●), porcine pancreatic PLA_2 (△), and porcine K116E (▲) mutant at 25 °C. The concentrations of proteins were 10 μM in 0.1 M phosphate buffer, pH 7.4. The f_u values were calculated from the θ_{222} values as described under Materials and Methods. The theoretical curves were constructed using the ΔG_{fold} and m values determined from the nonlinear least-squares analysis of data. $hpPLA_2$ and all other mutants (and $ppPLA_2$ and its mutants) have essentially the same ΔG_{fold} and m values.

Kinetic and Membrane Binding Properties of $hpPLA_2$ Mutants. To systematically determine the effects of the mutations on the interfacial catalysis of $hpPLA_2$, we measured the affinity of wild type and mutants for polymerized liposomes and their activity toward various phospholipid substrates. We previously showed that the changes in interfacial affinity could be accurately determined using

Table 1: Kinetic and Binding Parameters of hpPLA$_2$ and Mutants

	$(k_{cat}/K_m)_{app}$[a] (M^{-1} s^{-1})					
enzymes	diC_6PG monomers	diC_8PC micelles	TX/DC/diC_8PE micelles[c]	pyrene-PE/BLPG-polymerized mixed liposomes	pyrene-PG/BLPG-polymerized mixed liposomes	nK_d[b] (μM) BLPG-polymerized liposomes
WT	$(7.0 \pm 0.2) \times 10^3$	$(1.3 \pm 0.2) \times 10^5$	$(8.3 \pm 0.2) \times 10^4$	$(3.3 \pm 0.5) \times 10^6$	$(2.2 \pm 0.5) \times 10^6$	8 ± 3
R6E	$(6.0 \pm 0.1) \times 10^3$	$(6.8 \pm 0.5) \times 10^4$	$(2.8 \pm 0.2) \times 10^4$	$(2.5 \pm 0.5) \times 10^5$	$(7.0 \pm 1.0) \times 10^4$	80 ± 20
K7E	$(3.0 \pm 0.2) \times 10^3$	$(3.5 \pm 0.8) \times 10^4$	$(1.7 \pm 0.2) \times 10^4$	$(1.5 \pm 0.5) \times 10^5$	$(3.3 \pm 0.5) \times 10^4$	80 ± 20
K10E	$(6.5 \pm 0.3) \times 10^3$	$(7.2 \pm 0.9) \times 10^4$	$(3.0 \pm 0.2) \times 10^4$	$(2.3 \pm 0.6) \times 10^5$	$(8.2 \pm 1.0) \times 10^4$	70 ± 10
D53K	$(1.0 \pm 0.1) \times 10^4$	$(1.2 \pm 0.2) \times 10^4$	$(6.6 \pm 0.2) \times 10^3$	$(3.3 \pm 0.3) \times 10^5$	$(5.1 \pm 0.2) \times 10^6$	13 ± 4
K56E	$(3.0 \pm 0.2) \times 10^3$	$(1.5 \pm 0.2) \times 10^5$	$(1.0 \pm 0.2) \times 10^5$	$(3.8 \pm 0.5) \times 10^6$	$(6.1 \pm 0.1) \times 10^5$	11 ± 3
K116E	$(1.0 \pm 0.1) \times 10^3$	$(2.1 \pm 0.3) \times 10^3$	$(1.2 \pm 0.5) \times 10^3$	$(1.5 \pm 0.2) \times 10^4$	$(1.4 \pm 1.0) \times 10^4$	290 ± 50

[a] The $(k_{cat}/K_M)_{app}$ values represent mean value $\pm$ SD determined from three measurements. [b] The nK_d values represent best fit value $\pm$ SD determined from the nonlinear least-squares analyses of data. [c] Triton X-100/sodium deoxycholate/diC_8PE (4:2:1) mixed micelles.

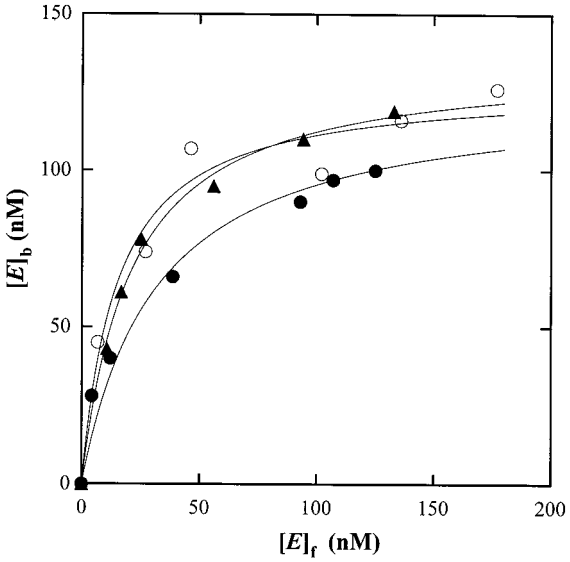

FIGURE 3: Binding isotherms of human pancreatic PLA$_2$ (○), D53K (●), and K56E (▲). The binding assay buffers contained 10 mM Tris-HCl buffer, pH 7.4, 0.16 M NaCl, 10 mM $CaCl_2$, and 100 μM BLPG-polymerized liposomes. The solid lines indicate theoretical curves constructed using eq 1 with the n and K_d values determined from the nonlinear least-squares analyses.

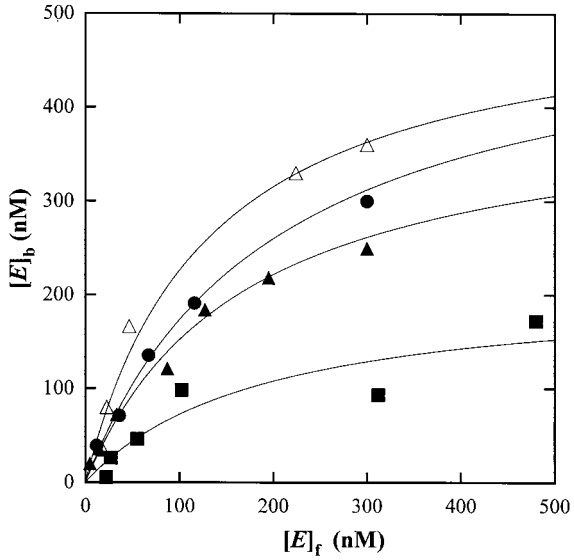

FIGURE 4: Binding isotherms of human pancreatic PLA$_2$ mutants including R6E (●), K7E (△), K10E (▲), and K116E (■). Experimental conditions were the same as described for Figure 3 except that the bulk BLPG concentrations were 200 μM for R6E and K10E and 300 μM for K7E and K116E.

nonhydrolyzable polymerized liposomes (*11*, *16*, *22*). All the mammalian pancreatic PLA$_2$s strongly prefer anionic interfaces to zwitterionic ones (*8*). To quantitatively determine the contributions of mutated residues to the energetics of the interfacial binding of hpPLA$_2$, equilibrium dissociation constants were determined for wild type and mutants using anionic BLPG-polymerized liposomes. Binding isotherms are illustrated in Figures 3 and 4. Because they all show a saturation binding pattern, the data were analyzed using a simple Langmuir type equation assuming the presence of the enzyme binding sites composed of n phospholipids on the liposome surface. Note that K_d reflects the molarity of these enzyme binding sites, and, thus, nK_d is the dissociation constant in terms of molarity of single lipid molecules. The nK_d values determined from the curve fitting of binding data to eq 1 (see Materials and Methods) are listed in Table 1. All three mutations in the amino terminus resulted in ca. 10-fold increases in nK_d, indicating that the three cationic residues (Arg-6, Lys-7, Lys-10) make significant and comparable contributions to the binding of hpPLA$_2$ to anionic membranes. Another cationic residue in the carboxy terminus, Lys-116, also appears to be important for interfacial binding as its mutation resulted in the largest 30-fold reduction in interfacial affinity. In contrast, the mutations in the putative substrate binding site (D53K and K56E) had no significant effect on interfacial binding. Together, the binding data indicate that Arg-6, Lys-7, Lys-10, and Lys-116 are involved in the binding of hpPLA$_2$ to anionic membranes.

We then measured the enzymatic activity of hpPLA$_2$ and mutants toward polymerized mixed liposomes. We previously showed that the changes in interfacial enzyme activity of bpPLA$_2$ could be sensitively detected using polymerized mixed liposomes as substrates (*8*). In a polymerized mixed liposome system, it is also possible to accurately determine the headgroup specificity of PLA$_2$ by varying the headgroup structure of hydrolyzable phospholipids in an inert polymerized matrix (*11*, *16*). Two phospholipids, pyrene-PE and pyrene-PG, were used as inserts in the BLPG-polymerized matrix. If the altered activity of a mutant toward polymerized mixed liposomes is solely due to its altered liposome affinity, then the relative activity of mutants should directly reflect the relative population of the liposome-bound enzyme. The values of $[E]_{bound}/[E]_{total}$ for individual mutants can be estimated from their nK_d values using the equation: $[E]_{bound}/[E]_{total} = 1/(1 + nK_d/[BLPG]_T)$ when $[BLPG]_T \gg n[E]_{total}$. For instance, the percent of membrane-bound K116E was

18 times lower than that of the wild-type enzyme under our kinetic conditions ($[BLPG]_T = 10\ \mu M$; see Materials and Methods). Similarly, R6E, K7E, and K10E had about 5-fold lower population of membrane-bound proteins than did wild type. Note that these estimates are all smaller than the decreases in their activity toward pyrene-PG/BLPG-polymerized mixed liposomes, which ranges from 200-fold for K116E to 30-fold for R6E and K10E (70-fold for K7E). This discrepancy would suggest that the mutation might reduce not only the interfacial binding affinity but also the catalytic efficiency of the enzyme.

The wild-type $hpPLA_2$ slightly favored pyrene-PE to pyrene-PG in polymerized mixed liposomes, which is unique among pancreatic PLA_2s that normally have a strong preference for an anionic PG substrate (*12*). All the IBS mutants of $hpPLA_2$, R6E, K7E, K10E, and K116E, exhibited essentially the same headgroup specificity, indicating that Arg-6, Lys-7, Lys-10, and Lys-116 are not directly involved in the interaction with the phospholipid headgroup. In contrast, D53K and K56E mutations had differential effects on the activity of $hpPLA_2$ toward pyrene-PE and pyrene-PG in polymerized mixed liposomes. D53K showed 10-fold lower activity than wild type toward pyrene-PE but 2.5-fold higher activity than wild type toward pyrene-PG. On the other hand, K56E was 1.2-fold more active than wild type toward pyrene-PE but 4-fold less active than wild type toward pyrene-PG. Note that the two mutations had minimal effects on the affinity of $hpPLA_2$ for BLPG. Thus, these data clearly indicate that Asp-53 favorably interacts with the cationic headgroup of the active-site-bound pyrene-PE and that Lys-56 is involved in interaction with the PG headgroup.

To figure out the cause for the unexpectedly low interfacial activity of IBS mutants of $hpPLA_2$, we measured the activity of wild type and mutants toward diC_6PG monomers. The substrate concentration, 0.5 mM, is well below the critical micelle concentration for this short-chain phospholipid (ca. 7 mM) (*24*). Although the premicellar aggregation of short-chain phospholipids with some PLA_2s has been reported (*25*), it is generally thought that the pancreatic PLA_2-catalyzed hydrolysis of these substrates below the critical micellar concentration does not involve interfacial binding. Thus, the relative activity of mutants toward diC_6PG monomers versus wild-type $hpPLA_2$ would reflect the changes in the catalytic efficiency and the substrate headgroup specificity of the active site. The values of $(k_{cat}/K_M)_{app}$ determined from reaction progress curves are summarized in Table 1. Among the mutants of IBS residues, K7E and K116E showed 2.3-fold and 7-fold decreases in activity whereas R6E and K10E were essentially as active as wild type. This accounts for why the former mutants showed significant lower activity than the latter toward polymerized mixed liposomes. This still does not fully explain, however, why all four mutants exhibited lower activity toward polymerized mixed liposomes than expected from their liposome affinity. In accordance with the kinetic data on polymerized mixed liposomes, the mutations of Asp-53 and Lys-56 had opposite effects on the activity of $hpPLA_2$ on diC_6PG, corroborating that Asp-53 repels a PG substrate whereas Lys-56 interacts favorably with it.

We then measured the activity of $hpPLA_2$ and mutants toward Triton X-100/sodium deoxycholate/diC_8PE (4:2:1) mixed micelles to further elucidate the origin of the low interfacial activity of IBS mutants. We previously reported that phospholipids dispersed in the anionic mixed micelles of Triton X-100/sodium deoxycholate are good substrates for pancreatic PLA_2s because of the anionic surface charge and the relatively loose surface packing density of these micelles (*8, 21*). As summarized in Table 1, the amino-terminal mutants were only modestly less active than wild type toward the mixed micelles, with K7E showing the lowest activity. This suggests that the binding of $hpPLA_2$ to mixed micelles depends less on the IBS cationic residues. However, a drastic decrease in activity was seen with K116E (60-fold), implying that Lys-116 might play a special role in the interfacial catalysis of $hpPLA_2$ toward mixed micelles. Finally, the effects of D53K and K56E mutations on the activity of $hpPLA_2$ toward the mixed micelles were in line with those seen with pyrene-PE/BLPG-polymerized mixed liposomes, showing that the effects mainly derive from altered substrate binding.

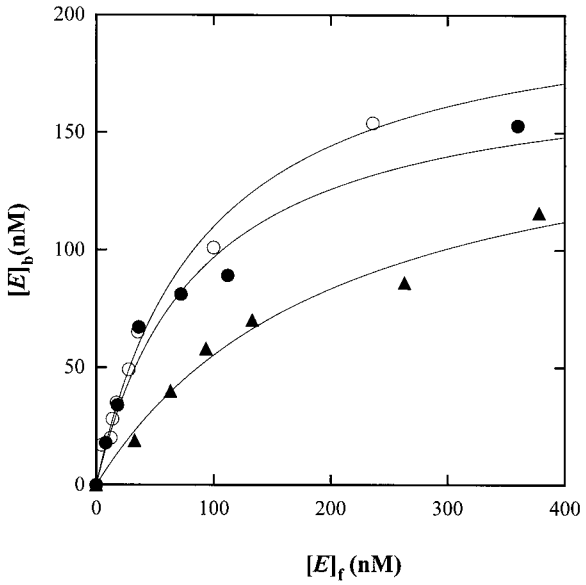

FIGURE 5: Binding isotherms of porcine pancreatic PLA_2 mutants including R6E (○), K10E (●), and K116E (▲). Experimental conditions were the same as described for Figure 3. The binding data of wild type are not shown because of the difference in the data scale.

Kinetic and Membrane Binding Properties of $ppPLA_2$ Mutants. To see whether $ppPLA_2$ binds to the membrane surface in a similar mode, we determined the kinetic and membrane binding properties of $ppPLA_2$ and its mutants. We first measured the affinity of these proteins for BLPG-polymerized liposomes. Binding isotherms are shown in Figure 5 and the nK_d values determined from curve fitting are listed in Table 2. The nK_d value of $ppPLA_2$ is ca. 3.5-fold lower than that of $hpPLA_2$, which is consistent with the higher activity of the former toward polymerized mixed liposomes (*12*). The effects of R6E, K10E, and K116E mutations on the interfacial binding affinity of $ppPLA_2$ are 2−4 times larger than those seen with their human counterparts. In contrast, K56E bound polymerized liposomes as tightly as wild type, showing that Lys-56 is not involved in interfacial binding. We then measured the activity of $ppPLA_2$ and its mutants toward polymerized mixed liposomes. For R6E, K10E, and K116E, decreases in activity toward polymerized mixed liposomes were comparable to or smaller than those in affinity for polymerized liposomes. This, which

Table 2: Kinetic and Binding Parameters of $ppPLA_2$ and Mutants

	$(k_{cat}/K_m)_{app}$[a] ($M^{-1}\,s^{-1}$)				
enzymes	diC_6PG monomers	TX/DC/diC_8PE micelles[c]	pyrene-PE/BLPG-polymerized mixed liposomes	pyrene-PG/BLPG-polymerized mixed liposomes	nK_d[b] (μM) BLPG-polymerized liposomes
WT	$(5.0 \pm 0.1) \times 10^3$	$(2.8 \pm 0.2) \times 10^4$	$(3.1 \pm 1.0) \times 10^6$	$(1.4 \pm 0.2) \times 10^7$	2.3 ± 1.0
R6E	$(5.0 \pm 0.1) \times 10^3$	$(1.1 \pm 0.1) \times 10^4$	$(3.0 \pm 1.2) \times 10^5$	$(1.4 \pm 0.2) \times 10^6$	90 ± 5
K10E	$(7.0 \pm 0.2) \times 10^3$	$(1.0 \pm 0.2) \times 10^4$	$(3.1 \pm 1.5) \times 10^5$	$(1.0 \pm 0.1) \times 10^6$	47 ± 2
K56E	$(2.0 \pm 0.2) \times 10^3$	$(6.7 \pm 0.1) \times 10^4$	$(5.3 \pm 0.7) \times 10^6$	$(8.0 \pm 1.5) \times 10^6$	2.3 ± 1.0
K116E	$(0.8 \pm 0.1) \times 10^3$	$(4.0 \pm 0.5) \times 10^2$	$(4.5 \pm 2.0) \times 10^4$	$(2.3 \pm 0.2) \times 10^5$	120 ± 20

[a] The $(k_{cat}/K_M)_{app}$ values represent mean value $\pm$ SD determined from three measurements. [b] The nK_d values represent best fit value $\pm$ SD determined from the nonlinear least-squares analyses of data. [c] Triton X-100/sodium deoxycholate/diC_8PE (4:2:1) mixed micelles.

is in contrast to the kinetic properties of $hpPLA_2$ mutants, suggests that the reduced activity of these mutants largely reflects the decreased interfacial binding affinity. Also, these mutants and wild type prefer pyrene-PG to pyrene-PE to comparable degrees, indicating that Arg-6, Lys-10, and Lys-116 are not involved in substrate binding. In contrast, K56E had modestly enhanced activity toward pyrene-PE and reduced activity toward pyrene-PG, indicating its involvement in substrate binding.

We then measured the activity of $ppPLA_2$ and mutants toward diC_6PG monomers and Triton X-100/sodium deoxycholate/diC_8PE (4:2:1) mixed micelles. As was the case with $hpPLA_2$, K116E displayed a 6.3-fold decrease in activity toward diC_6PG monomers, suggesting that the mutation also impairs the catalytic efficiency of $ppPLA_2$. On the other hand, R6E and K10E had the full wild-type activity. Also, K56E showed the decreased activity which was comparable with that seen with pyrene-PG/BLPG-polymerized mixed liposomes. Toward the mixed micelles, R6E and K10E had modestly decreased activity whereas K116E showed a drastic 70-fold reduction in activity, which is similar to the finding with their human counterparts. K56E was more active than wild type, as expected from its higher activity toward pyrene-PE/BLPG-polymerized mixed liposomes. Taken together, these results indicate that Arg-6, Lys-10, and Lys-116 of $ppPLA_2$ are important in its binding to anionic interfaces and that Lys-56 is involved in interaction with an active-site-bound substrate.

DISCUSSION

This report describes a comparative analysis of the interfacial binding and substrate binding modes of $hpPLA_2$ and $ppPLA_2$. In conjunction with our previous studies on $bpPLA_2$ (*8*), this study thus reveals similarities and differences in the mechanisms by which mammalian pancreatic PLA_2s interact with lipid aggregates and catalyze the lipid hydrolysis. An earlier crystallographic study of $bpPLA_2$ predicted that its IBS is composed of the residues clustered in the amino and carboxy termini and several other residues (*26*). Previous structure−function studies of $bpPLA_2$ indicated that Lys-10, Lys-56, and Lys-116 are involved in electrostatic interactions with anionic interfaces (*8*) and Trp-3 and Leu-20 in nonelectrostatic interfacial interactions (*9*, *13*). The present study shows that $hpPLA_2$ and $ppPLA_2$ have similar interfacial binding modes, which are different from that of $bpPLA_2$. Apparently, the most striking difference is the critical involvement of Lys-56 in the interfacial binding of $bpPLA_2$, the origin of which is the subject of the accompanying paper (*30*). Lys-56 plays no role in the interfacial binding of $hpPLA_2$ and $ppPLA_2$. The three pancreatic PLA_2s, however, share some common traits in that cationic residues in the amino terminus and Lys-116 in the carboxy terminus are involved in the interfacial binding of all these PLA_2s. Between $hpPLA_2$ and $ppPLA_2$, small but definite differences are noted in the interfacial binding mode and in the contribution of each cationic residue to interfacial binding.

Our binding measurements show that the cationic residues in the putative IBS of $hpPLA_2$ and $ppPLA_2$ make significant individual contributions to overall interfacial binding. These cationic residues include Arg-6, Lys-7, Lys-10, and Lys-116 for $hpPLA_2$ and Arg-6, Lys-10, and Lys-116 for $ppPLA_2$. Using the equation $\Delta\Delta G^\circ = RT \ln [nK_d(\text{wild type})/nK_d(\text{mutant})]$, one can estimate that the mutations of the amino-terminal residues of $hpPLA_2$ decrease the free energy of binding to anionic liposomes by 1.3 kcal/mol under the standard conditions whereas the K116E mutation reduces the energy by 2.1 kcal/mol. These energy values compare well with the energy contributions from the cationic IBS residues of $bpPLA_2$ (*8*) and *Agkistrodon piscivorus piscivorus* PLA_2 (*10*). For $ppPLA_2$, individual contributions are larger: the R6E and K116E mutations decrease the binding energy by 2.3 kcal/mol and the K10E mutation by 1.8 kcal/mol. We previously reported that despite comparable interfacial affinity, the individual contributions of the IBS cationic residues of human group IIa PLA_2 to interfacial binding are considerably smaller than those of *A. p. piscivorus* PLA_2, because the former contains a much larger number of cationic residues on its IBS than the latter (*22*). Similarly, the lower individual contributions of the IBS residues of $hpPLA_2$ might simply reflect the fact that $hpPLA_2$ has the largest number of IBS cationic residues among the three pancreatic PLA_2s.

A unique finding about $hpPLA_2$ is that the charge-reversal mutations of its IBS cationic residues led to larger decreases in activity on polymerized mixed liposomes than expected from their reduced affinity for polymerized liposomes. This finding is not due to the artifacts inherent in our polymerized mixed liposome kinetic system, as corresponding $ppPLA_2$ mutants do not show the same behavior (see Table 2). Nor does it seem to be due to the deleterious conformational changes of the proteins as the mutants have similar CD spectra and thermodynamic stability as wild type. The most pronounced differences seen with K7E and K116E are in part due to the perturbation of the active site as indicated by significantly reduced activity toward diC_6PG monomers (2.3- and 7-fold reduction in catalytic efficiency, respectively).

Considering the remoteness of Lys-7 and Lys-116 from the active site, this effect might derive from either steric hindrance to active-site entry (for Lys-7) or a change in the electrostatic potential in the active site (for both lysines). A similar effect by remote cationic residues on the catalytic site has been reported for human group IIa PLA_2 (*22*). If this factor is taken into account, all four mutants (R6E, K7E, K10E, K116E) would show comparable 10−30-fold decreases in activity toward polymerized mixed liposomes, which is still larger than expected from their interfacial affinity. It has been indicated that PLA_2 molecules can bind to membrane surfaces in different orientations, only a limited selection of which are conducive to interfacial catalysis (*10*, *27*). Thus, it is possible that the low activity of the IBS mutants of $hpPLA_2$ is due to the enhanced proportion of liposome-bound mutants with nonproductive orientation. This notion in turn implies that the cationic IBS residues of $hpPLA_2$ might be involved not only in the initial interfacial adsorption of enzyme molecules but also in the proper orientation of liposome-bound enzymes. As shown in Tables 1 and 2, $ppPLA_2$ has significant higher interfacial activity and affinity than does $hpPLA_2$. Presumably, the orientational effect by cationic IBS residues is not as critical for $ppPLA_2$ that has significantly higher intrinsic activity for liposomal substrates. A similar argument can be used to account for the relative activity of $hpPLA_2$ mutants toward Triton X-100/sodium deoxycholate/diC_8PE (4:2:1) mixed micelles. All three amino-terminal mutations of $hpPLA_2$ modestly (2−3-fold) decrease its activity on mixed micelles. Since these micelles provide more loosely packed and less anionic surfaces for $hpPLA_2$ than do polymerized mixed liposomes, the interfacial binding might be less dependent on electrostatic interactions, and the requirement for the productive orientation of surface-bound PLA_2 might be less stringent.

The involvement of Lys-116 in the interfacial binding of $bpPLA_2$ was disputed, based on the unaltered activity of a $bpPLA_2$ mutant lacking the carboxy-terminal region (*28*). The finding that Lys-116 is also involved in the interfacial binding of $hpPLA_2$ and $ppPLA_2$ would, however, support the notion that this absolutely conserved cationic residue plays a significant role in the interfacial binding of pancreatic PLA_2s. The K116E mutants of both $hpPLA_2$ and $ppPLA_2$ show drastically reduced activity (70- and 130-fold decreases, respectively, compared to their wild-type enzymes) toward mixed micelles. This raises an interesting possibility that Lys-116 might be involved in the formation of enzyme−micelle complex, which has been proposed to occur in the interfacial catalysis of $ppPLA_2$ on micellar substrates (*29*). The formation of this complex, containing multiple enzyme and lipid molecules, appears to be distinct from the adsorption of PLA_2 to liposome surfaces (*29*). To further explore this possibility, we measured the activity of wild-type $hpPLA_2$ and mutants toward zwitterionic diC_8PC micelles. As listed in Table 1, K116E again showed a drastic 50-fold decrease in activity whereas other IBS mutants exhibited only modest changes in activity. Similar results were observed for both $bpPLA_2$ and $ppPLA_2$ (data not shown). Given that electrostatic forces would play a less important role in binding to zwitterionic surfaces of diC_8PC micelles, these results point to the involvement of Lys-116 in the formation of an enzyme−micelle complex. The insignificant effects of other mutations also suggest that the amino-terminal IBS residues would not be directly involved in this process. Further studies are needed to understand the relevance, mechanism, and physiological significance of the complex formation in the digestive actions of pancreatic PLA_2s.

As far as the substrate headgroup specificity is concerned, the unique specificity of $hpPLA_2$ can be accounted for in terms of electrostatic interactions between the charged side chains of residues 53 and 56 and the phospholipid headgroup. The BLAST search of the primary structures of mammalian pancreatic PLA_2s shows that $hpPLA_2$ is the only enzyme with an anionic residue in position 53. It has been shown that Lys-53 of $bpPLA_2$ (*8*) and Arg-53 of $ppPLA_2$ (*14*) are involved in favorable electrostatic interactions with the headgroup of active-site-bound anionic phospholipid. For $hpPLA_2$, Asp-53 appears to participate in stabilizing electrostatic interactions with the cationic ethanolamine headgroup, hence the modest PE preference. The physiological significance of this substrate specificity of $hpPLA_2$ in terms of the digestion of dietary phospholipids remains to be elucidated. For all three pancreatic PLA_2s, Lys-56 seems to be involved in stabilizing interactions with the headgroup of anionic phospholipids. Since Lys-56 is absolutely conserved among mammalian pancreatic PLA_2s, it is expected that all pancreatic enzymes will effectively catalyze the hydrolysis of anionic phospholipids.

REFERENCES

1. Dennis, E. A. (1997) *Trends Biochem. Sci. 22*, 1−2.
2. Waite, M. (1987) *The Phospholipases*, Plenum Press, New York.
3. Tohkin, M., Kishino, J., Ishizaki, J., and Arita, H. (1993) *J. Biol. Chem. 268*, 2865−2871.
4. Jain, M. K., and Berg, O. G. (1989) *Biochim. Biophys. Acta 1002*, 127−156.
5. Gelb, M. H., Jain, M. K., Hanel, A. M., and Berg, O. G. (1995) *Annu. Rev. Biochem. 64*, 653−688.
6. Scott, D. L., and Sigler, P. B. (1994) *Adv. Protein Chem. 45*, 53−88.
7. Scott, D. L., White, S. P., Otwinowski, Z., Gelb, M. H., and Sigler, P. B. (1990) *Science 250*, 1541−1546.
8. Dua, R., Wu, S.-K., and Cho, W. (1995) *J. Biol. Chem. 270*, 263−268.
9. Lee, B.-I., Yoon, E. T., and Cho, W. (1996) *Biochemistry 35*, 4231−4240.
10. Han, S.-K., Yoon, E. T., Scott, D. L., Sigler, P. B., and Cho, W. (1997) *J. Biol. Chem. 272*, 3573−3582.
11. Wu, S.-K., and Cho, W. (1993) *Biochemistry 32*, 13902−13908.
12. Han, S.-K., Lee, B.-I., and Cho, W. (1997) *Biochim. Biophys. Acta 1346*, 185−192.
13. Liu, X., Zhu, H., Huang, B., Rogers, J., Yu, B. Z., Kumar, A., Jain, M. K., Sundaralingam, M., and Tsai, M. D. (1995) *Biochemistry 34*, 7322−7334.
14. Lugtigheid, R. B., Otten-Kuipers, M. A., Verheij, H. M., and De Haas, G. H. (1993) *Eur. J. Biochem. 213*, 517−522.
15. Kuipers, O. P., Kerver, J., van Meersbergen, J., Vis, R., Dijkman, R., Verheij, H. M., and De Haas, G. H. (1990) *Protein Eng. 3*, 599−603.
16. Wu, S.-K., and Cho, W. (1994) *Anal. Biochem. 221*, 152−159.
17. Kates, M. (1986) *Techniques of Lipidology*, 2nd ed., Elsevier, Amsterdam.
18. Thannhauser, T. W., Konishi, Y., and Scheraga, H. A. (1984) *Anal. Biochem. 138*, 181−188.
19. Pace, C. N. (1986) *Methods Enzymol. 131*, 266−280.

20. Santoro, M. M., and Bolen, D. W. (1988) *Biochemistry 27*, 8063−8068.
21. Dua, R., and Cho, W. (1994) *Eur. J. Biochem. 221*, 481−490.
22. Snitko, Y., Koduri, R., Han, S.-K., Othman, R., Baker, S. F., Molini, B. J., Wilton, D. C., Gelb, M. H., and Cho, W. (1997) *Biochemistry 36*, 14325−14333.
23. Snitko, Y., Yoon, E. T., and Cho, W. (1997) *Biochem. J. 321*, 737−741.
24. Wells, M. A. (1974) *Biochemistry 13*, 2248−2257.
25. Yuan, W., Quinn, D. M., Sigler, P. B., and Gelb, M. H. (1990) *Biochemistry 29*, 6082−6094.
26. Dijkstra, B. W., Drenth, J., and Kalk, K. H. (1981) *Nature 289*, 604−606.
27. Burack, W. R., and Biltonen, R. L. (1994) *Chem. Phys. Lipids 73*, 209−222.
28. Huang, B., Yu, B. Z., Rogers, J., Byeon, I. J., Sekar, K., Chen, X., Sundaralingam, M., Tsai, M. D., and Jain, M. K. (1996) *Biochemistry 35*, 12164−12174.
29. de Araujo, P. S., Rosseneu, M. Y., Kremer, J. M., van Zoelen, E. J., and de Haas, G. H. (1979) *Biochemistry 18*, 580−586.
30. Lee, B. I., Dua, R., and Cho, W. (1999) *Biochemistry 38*, 7811−7818.

BI990600E